BRAIN
ORIGINAL ARTICLE

Extracellular vesicle biomarkers for cognitive impairment in Parkinson's disease

Joseph Blommer,[1,†] Toni Pitcher,[2,3,†] Maja Mustapic,[1] Erden Eren,[1] Pamela J. Yao,[1] Michael P. Vreones,[1] Krishna A. Pucha,[1] John Dalrymple-Alford,[2,4] Reza Shoorangiz,[2] Wassilios G. Meissner,[2,5,6] Tim Anderson[2,3,‡] and Dimitrios Kapogiannis[1,‡]

[†,‡]These authors contributed equally to this work.

Besides motor symptoms, many individuals with Parkinson's disease develop cognitive impairment perhaps due to coexisting α-synuclein and Alzheimer's disease pathologies and impaired brain insulin signalling. Discovering biomarkers for cognitive impairment in Parkinson's disease could help clarify the underlying pathogenic processes and improve Parkinson's disease diagnosis and prognosis.

This study used plasma samples from 273 participants: 103 Parkinson's disease individuals with normal cognition, 121 Parkinson's disease individuals with cognitive impairment (81 with mild cognitive impairment, 40 with dementia) and 49 age- and sex-matched controls. Plasma extracellular vesicles enriched for neuronal origin were immunocaptured by targeting the L1 cell adhesion molecule, then biomarkers were quantified using immunoassays.

α-Synuclein was lower in Parkinson's disease compared to control individuals ($P = 0.004$) and in cognitively impaired Parkinson's disease individuals compared to Parkinson's disease with normal cognition ($P < 0.001$) and control ($P < 0.001$) individuals. Amyloid-β_{42} did not differ between groups. Phosphorylated tau (T181) was higher in Parkinson's disease than control individuals ($P = 0.003$) and in cognitively impaired compared to cognitively normal Parkinson's disease individuals ($P < 0.001$) and controls ($P < 0.001$). Total tau was not different between groups. Tyrosine-phosphorylated insulin receptor substrate-1 was lower in Parkinson's disease compared to control individuals ($P = 0.03$) and in cognitively impaired compared to cognitively normal Parkinson's disease individuals ($P = 0.02$) and controls ($P = 0.01$), and also decreased with increasing motor symptom severity ($P = 0.005$); serine312-phosphorylated insulin receptor substrate-1 was not different between groups. Mechanistic target of rapamycin was not different between groups, whereas phosphorylated mechanistic target of rapamycin trended lower in cognitively impaired compared to cognitively normal Parkinson's disease individuals ($P = 0.05$). The ratio of α-synuclein to phosphorylated tau181 was lower in Parkinson's disease compared to controls ($P = 0.001$), in cognitively impaired compared to cognitively normal Parkinson's disease individuals ($P < 0.001$) and decreased with increasing motor symptom severity ($P < 0.001$). The ratio of insulin receptor substrate-1 phosphorylated serine312 to insulin receptor substrate-1 phosphorylated tyrosine was higher in Parkinson's disease compared to control individuals ($P = 0.01$), in cognitively impaired compared to cognitively normal Parkinson's disease individuals ($P = 0.02$) and increased with increasing motor symptom severity ($P = 0.003$). α-Synuclein, phosphorylated tau181 and insulin receptor substrate-1 phosphorylated tyrosine contributed in diagnostic classification between groups.

These findings suggest that both α-synuclein and tau pathologies and impaired insulin signalling underlie Parkinson's disease with cognitive impairment. Plasma neuronal extracellular vesicles biomarkers may inform cognitive prognosis in Parkinson's disease.

1 National Institute on Aging, Intramural Research Program, Laboratory of Clinical Investigation, Baltimore, MD 21224, USA
2 New Zealand Brain Research Institute, Christchurch 8011, New Zealand

Received October 14, 2021. Revised January 24, 2022. Accepted June 22, 2022. Advance access publication July 14, 2022
Published by Oxford University Press on behalf of the Guarantors of Brain 2022.

3 Department of Medicine, University of Otago, Christchurch 8011, New Zealand
4 School of Psychology, Speech and Hearing, University of Canterbury, Christchurch 8041, New Zealand
5 University of Bordeaux, CNRS, IMN, UMR 5293, F-33000 Bordeaux, France
6 Service de Neurologie—Maladies Neurodégénératives, CHU Bordeaux, F-33000 Bordeaux, France

Correspondence to: Dimitrios Kapogiannis, MD
Laboratory of Clinical Investigation
National Institute on Aging
251 Bayview Blvd, Baltimore, MD 21224, USA
E-mail: kapogiannisd@mail.nih.gov

Correspondence may also be addressed to: Tim Anderson, MD
New Zealand Brain Research Institute
66 Stewart Street, Christchurch, Christchurch 8011, New Zealand
E-mail: Tim.Anderson@cdhb.health.nz

Keywords: Parkinson's disease; biomarkers; extracellular vesicles; synuclein; tau; insulin signalling

Introduction

Parkinson's disease is the second most common neurodegenerative disease and is characterized by bradykinesia, resting tremor, rigidity and postural instability.[1,2] The loss of dopaminergic neurons in the substantia nigra pars compacta and the accumulation of α-synuclein forming Lewy bodies are the neuropathological hallmark of Parkinson's disease.[3,4] While classic motor symptoms are key to the clinical diagnosis of Parkinson's disease, many patients also experience progressive cognitive impairment (PD-CI), including those with mild cognitive impairment (PD-MCI) and dementia (PDD).[5] The heterogeneity of clinical presentations in Parkinson's disease makes it important to develop biomarkers to improve the accuracy of disease diagnosis and prognosis and potentially stratify for future therapeutic strategies based on personalized medicine.

The spread of α-synuclein pathology in subcortical and cortical regions besides the substantia nigra is believed to lead to widespread neurodegeneration and cognitive decline. Some pathological studies of PDD individuals have identified α-synuclein pathology in multiple brain regions, yet other studies have found that some PDD individuals have minimal cortical α-synuclein pathology.[6] Additionally, some Parkinson's disease individuals show significant Lewy body pathology without ever developing dementia. This suggests that α-synuclein pathology is not exclusively responsible for the development of cognitive impairment in Parkinson's disease. Interestingly, Alzheimer's disease-associated aggregating proteins amyloid-β (Aβ) and tau are also present concomitantly with α-synuclein pathology in Parkinson's disease,[7,8] with clinicopathologic evidence suggesting that a combined metric of Lewy body, Aβ and tau pathologies is the best correlate of dementia in Parkinson's disease. Moreover, a growing body of literature implicates abnormal insulin signalling in Parkinson's disease pathogenesis, as a factor exacerbating the pathological features of Parkinson's disease.[9] Importantly, peripheral insulin resistance has been associated with increased non-motor symptoms in Parkinson's disease including cognitive impairment. α-Synuclein, Aβ, and tau pathologies and neuronal insulin resistance may be useful in identifying individuals with cognitive impairment in Parkinson's disease.

Extracellular vesicles (EVs) are membranous nanoparticles that are constitutively secreted by all cells including neurons.[10] The role of EVs in the brain includes the exchange of cargo molecules from cell to cell as a signalling mechanism, but also the trans-cellular spread of pathogenic proteins including α-synuclein, Aβ and phosphorylated tau.[11,12] EVs from the brain can cross the brain–blood barrier and a population of neuronal origin-enriched EVs (NEVs) can be isolated from peripheral blood using an immunocapture technique targeting the neuronal marker L1CAM (L1 cell adhesion molecule).[13–15] Our group and others have demonstrated the capacity of NEVs to yield biomarkers for clinical and preclinical diagnosis, prognosis and as a means of investigating disease mechanisms for neurodegenerative diseases, such as Alzheimer's disease and Parkinson's disease.[15–17]

In this study, we examined the ability of plasma NEV biomarkers to distinguish between healthy controls and Parkinson's disease individuals, as well as between PD-CI individuals and those with normal cognition (PD-N). We addressed two distinct hypotheses: (i) NEV cargo of aggregating proteins involved in Parkinson's disease and Alzheimer's disease [α-synuclein, Aβ42, total tau (tTau) and phosphorylated tau threonine181 (pTau181)] can distinguish between Parkinson's disease and control individuals and show stepwise differences between PD-N and PD-CI individuals, either PD-MCI or PDD; and (ii) NEV biomarkers indicating diminished canonical insulin signalling with decreased levels of insulin receptor substrate-1 phosphorylated tyrosine (pY-IRS-1, a facilitator of forward signal propagation) and/or increased levels of insulin receptor substrate-1 phosphorylated serine312 (pSer312-IRS-1, indicating insulin resistance)[18] can distinguish between Parkinson's disease and control individuals and between PD-N and PD-CI (PD-MCI and PDD) individuals. The canonical insulin signalling cascade feeds into the mechanistic target of rapamycin (mTOR) cascade; hence, we also explored differences in the phosphorylated mechanistic target of rapamycin (pmTOR). Finally, we sought to identify NEV biomarker associations with scales of disease severity and clinical measures.

Materials and methods

Participants

A convenience sample of individuals with Parkinson's disease was recruited through a Specialist Movement Disorders Clinic in Christchurch, New Zealand (TJA) into the New Zealand Parkinson's Progression Programme longitudinal study (Supplementary Fig. 1). Exclusions included dementia with Lewy

bodies, atypical parkinsonism and other major neurological or psychiatric conditions (e.g. stroke, major depression within 6 months, moderate to severe head injury and early life learning disability) or poor English, which would preclude testing. Healthy population controls were recruited from the local community, with the same exclusions applied. All participants underwent a series of assessments that meet the Level II MDS-PD-MCI Task Force criteria.[19] Mild cognitive impairment was defined using the cut-off of 1.5 standard deviations below normative data and dementia as significant impairment across at least two domains and displaying impairment in daily activities.[20] Clinical staging of Parkinson's disease was completed using the Movement Disorders Society Unified Parkinson's Disease Rating Scale (MDS-UPDRS) part III and the Hoehn and Yahr scale. Parkinson's medications were converted into a daily levodopa equivalent dose (LED) using established conversions.[21] A more detailed description of the study population and the neuropsychological tests used has been published previously.[22,23]

NEV isolation

Venous blood samples were collected in the morning (9 a.m. to 12 p.m.) using EDTA tubes and were processed into plasma by centrifugation (4°C) for 10 min at 2000*g*. Aliquots were stored at −80°C until shipment to the National Institute on Aging. NEV isolation was conducted blindly by National Institute on Aging investigators as described by Mustapic *et al.*[13] with minor modifications (Supplementary material). Briefly, plasma samples were defibrinated with thrombin, then total particles were precipitated using Exoquick® solution and NEVs were immunoprecipitated using antibodies against neuronal marker L1CAM. L1CAM+ NEVs were lysed and stored at −80°C until immunoassays.

Cryogenic transmission electron microscopy

Cryogenic TEM (Cryo-TEM) of intact NEV (Fig. 1A) was completed in the Nanoscale and Microscale Research Centre of the University of Nottingham, UK. Sample preparation for Cryo-TEM was adapted from a protocol that has been published elsewhere.[24,25] We used Holey carbon TEM grids (EM Resolutions). NEV samples were left to adsorb onto the grids (5 µl/grid) for 2 min and then excess solution was removed using filters. The NEV samples were blotted for 1 s and frozen in liquid ethane using a Gatan CP3 plunge freezing unit (Ametek). The frozen samples were loaded to a Tecnai G2 Spirit BioTWIN, a 20–120 kV/LaB6 Transmission Electron Microscope, with Cryo-TEM carried out with an accelerating voltage of 100 kV. We obtained the images using an inbuilt Gatan SIS Megaview IV digital camera.

Nanoparticle tracking analysis

Nanoparticle tracking analysis (NTA) uses the properties of light scattering and Brownian motion to calculate EV particle size and concentration. 10 µl of intact L1CAM+ NEVs were diluted in phosphate-buffered saline (PBS) for NTA using Nanosight NS500 (Malvern). Particle concentration and size were calculated from five 20-s videos with the following settings: camera level 16, detection threshold 4 and a dilution ranging from 1:60 to 1:200 providing a range from 20 to 100 particles per frame (Fig. 1B).

Western blotting and single molecule array sample preparation

For western blots (WB) (Figs. 1C and 2A) and single molecule array (SIMOA®) (Fig. 2B and Supplementary Fig. 2) experiments, EVs were isolated from 0.5 ml of plasma of the same healthy volunteers using the described protocol (Supplementary material) with modifications. After particle precipitation with Exoquick® and resuspension in 0.7 ml of ultra-pure D-water containing protease and phosphatase inhibitors, we isolated different subpopulations of EVs, alternatively using 25 µg of streptavidin-coated beads only (i.e. with no conjugated antibody), beads conjugated with an equal mixture of three anti-tetraspanin antibodies [anti-CD81 (Ancell, #302-030), anti-CD63 (Abnova, #MAB15361) and anti-CD-9 (BD Pharmingen, #558749)], beads conjugated with the 5G3 clone of anti-CD171 antibody and beads conjugated with antibody against ASGR2 (LSBio, #LS-C396170), a surface marker expressed in the liver and not expressed in the brain (https://www.proteinatlas.org/ENSG00000161944-ASGR2/tissue).

Each sample was prepared for western blotting by mixing 10 µg (for Fig. 1C) or 2 µg of total protein (for Fig. 2A) with loading buffer and heating it for 5 min at 95°C, which was then loaded to a 4–12% Bis–Tris Nupage gel. PVDF membranes were incubated with primary antibody L1CAM (BD Biosciences, #554273), CD9 (BioLegend, #312102), GM130 (Abcam, #ab52649), Alix (Novus Biologicals, #NBP1-90201), CD81 (System Biosciences, #EXOAB-CD81A-1), CD9 (Abcam, #ab92726), followed by anti-species secondary antibody and visualized using ECL or Odyssey® CLx imaging system. Next to the samples we also loaded human brain lysate as a positive control.

ExoView analysis

We analysed L1CAM and tetraspanin co-expression in NEVs by ExoView R200 (Nanoview Biosciences) following the manufacturer's instructions (Fig. 2C and D). Briefly, NEV samples (50 µl) were incubated on a modified ExoView Tetraspanin chip in a 24-well plate for 16 h. Then, the chip was washed three times with 1× Solution A. Next, we added 250 µl detection antibodies anti-LICAM [CD171 Monoclonal Antibody (eBio5G3), PE, eBioscience] and anti-CD9 (CF 647) in blocking buffer for 1 h. The chip was then washed twice with solution A, three times with solution B and finally with DI water. After drying on absorbent paper, chips were scanned with Exoview R200 and the acquired images were analysed with ExoScan software (Nanoview Biosciences).

Immunofluorescence labelling and high-resolution microscopy

We immunolabelled NEVs (Fig. 2E) using a protocol optimized from a method described by Mondal *et al.*[26] Isolated EVs were permeabilized in 0.001% Triton X-100 (in PBS) for 5 min, then an equal volume of 20% polyethylene glycol (PEG, 10 000; Sigma #92897) was added to achieve a final concentration of 10% PEG. The mixture was centrifuged, and the EV-containing pellet was suspended in PBS. The following primary antibodies were added to the EV-containing suspension: L1CAM mouse antibody (ThermoFisher Scientific, clone 5G3, #14-1719-95); Alix rabbit antibody (Novus, #NBP1-90201); Vamp2 rabbit antibody (Synaptic Systems, #104008). All primary antibodies were used at 1:50. The EV–antibody mixtures were incubated overnight with gentle rocking at 4°C. After adding an equal volume of 20% PEG to the EV–antibody suspension

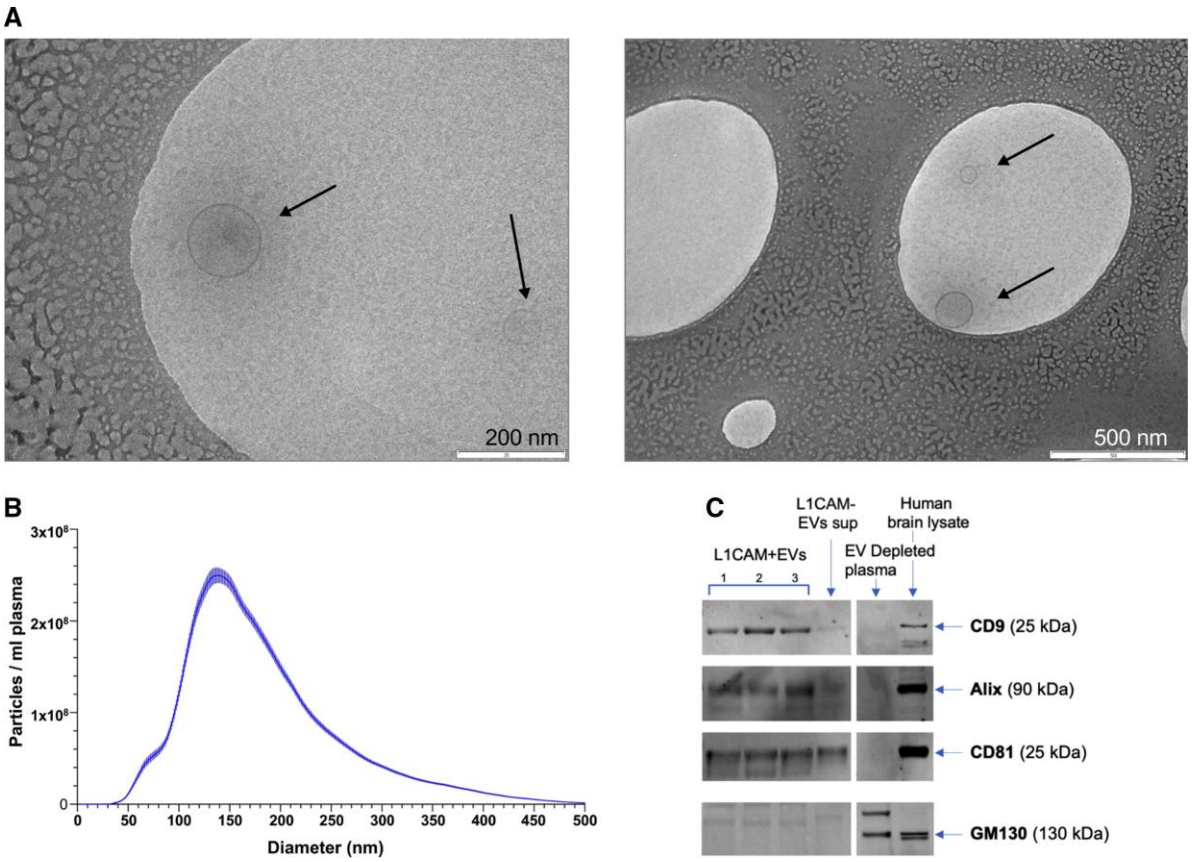

Figure 1 NEV characterization. (**A**) Characteristic cryo-TEM images of NEVs. (**B**) Graph depicts NEV concentration (NEV particles per ml) as a function of NEV diameter (determined using Nanoparticle Tracking Analysis). The blue line shows the average concentration at a given diameter and the shaded region shows the SEM of the concentration for that diameter across all study participants. (**C**) Western blots for intravesicular EV marker Alix and transmembrane EV markers CD9 and CD81 used as positive EV markers, and the *cis*-Golgi marker GM130 used as a negative EV marker. Lanes contain 10 µg of NEVs (L1CAM+ EVs, $n = 3$), supernatant after L1CAM immunoprecipitation (L1CAM-EVs sup, $n = 1$), EV-depleted plasma used as negative control for EV-specific markers ($n = 1$) and human brain lysate ($n = 1$). Visible western blot bands were quantified using LI-COR Image Studio software.

to achieve a final concentration of 10% PEG, the mixture was centrifuged, the supernatant was removed and the pellet was resuspended in PBS. The PEG precipitation of EVs was repeated three times and the resultant pellet was then suspended in PBS. Alexa Fluor 488 or 568 conjugated secondary antibodies (ThermoFisher Scientific) were added to the primary antibody-labelled EV suspension at 1:200 dilution, and the mixture was incubated for 1 h with gentle rocking in the dark. The mixture was then subjected to three rounds of PEG precipitation and wash (identical to the above steps for primary antibody), and the pellet containing immunolabelled EVs was suspended in 10–20 ml of PBS. Approximately 10 µl of labelled EVs was placed on a microscope slide and a small drop of mounting medium (ProLong antifade mountant; ThermoFisher Scientific) was added to the labelled EVs, and a glass coverslip (#1.5) was used to cover the EV–mounting medium mixture. Samples were imaged within 24 h after labelling using high-resolution microscopy (Airyscan module of Zeiss LSM800).

Immunoassays

To assess the amount of immunocaptured L1CAM+ EVs (Fig. 2B), we developed a homebrew intact L1CAM+ EV detection assay (SIMOA® technology). Briefly, intact EVs from different EV isolations were captured using a cocktail of three anti-tetraspanin antibodies (CD9/CD63/CD81). Captured EVs were detected using anti-L1CAM antibody. For quantification of EV cargo proteins, we used Meso Scale Diagnostics electrochemiluminescence assays to quantify α-synuclein (#K151WKK), pSer312-IRS-1 (#N450HLA), pY-IRS-1 (#N450HLA), mTOR (#N45170A) and pmTOR (#N45170A). We used a multiplexed magnetic bead assay from EMD Millipore to quantify Aβ42, pTau181 and tTau (#HNABTMAG-68K). All samples were run blindly in duplicate and coefficients of variance were determined. Rigorous quality control assessments and procedures were used to ensure data quality (Supplementary material).

Statistical analysis

Statistical analysis for western blots and intact L1CAM+ EV detection assay was performed using one-way ANOVA, followed by Tukey's multiple comparison test for pairwise comparisons (GraphPad Prism9).

For EV protein biomarkers, the measured analyte concentrations are presented in Supplementary Table 1, while log(10) transformed values are shown in plots and were used in statistics because the data were not normally distributed. Our analysis was primarily focused on comparing Parkinson's disease and control groups and secondarily on comparing PD-CI with PD-N and control groups. A further exploratory analysis compared control, PD-MCI, PDD and PD-N groups. Statistical analyses were performed in R (version 4.0.2). Plots were generated using ggplot2.[27] Group

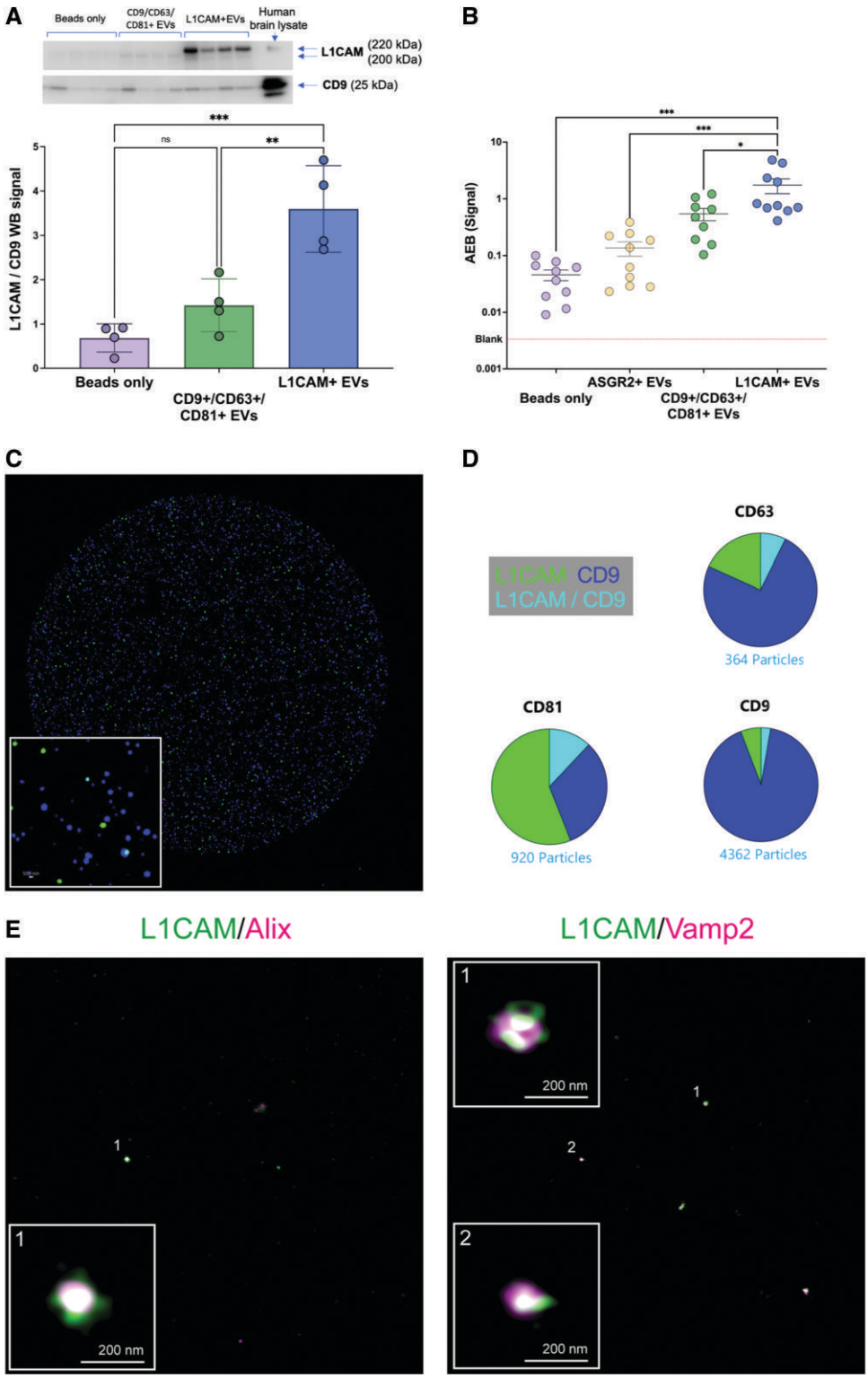

Figure 2 L1CAM immunoprecipitation yields a specific subpopulation of EVs. (**A**) Western blots for L1CAM and CD9 for validation of the L1CAM + EV immunoprecipitation. Using the same starting plasma samples, we conducted parallel isolations, which differed in the immunoprecipitation step, in terms of using 2 µg of beads only (i.e. not conjugated with antibody, $n = 3$); 2 µg of beads conjugated with a mix of anti-tetraspanin antibodies (i.e. yielding CD9+/CD63+/CD81+ EVs, $n = 3$); or 2 µg of beads conjugated with the 5G3 clone of anti-CD171 (L1CAM) antibody (i.e. L1CAM+ EVs, $n = 3$); human brain lysate used as a positive control; 10 µg of protein was loaded for each column. Horizontal labels and arrows indicate the probed target protein and band of interest at a particular molecular weight. Vertical arrows indicate sample labels. Visible western blot bands were quantified using AzureSpotPro software. Quantified values from L1CAM validation blots were statistically compared (one-way ANOVA) and graphed using GraphPad Prism software. The ratio of L1CAM/CD9 is higher for L1CAM+ EVs when compared to beads only or CD9+/CD63+/CD81+ EVs. (**B**) Results of novel homebrew SIMOA®-based assay for intact EVs (5G3 clone of anti-CD171 antibody used for capture, mix of anti-tetraspanin antibodies used for detection).

(Continued)

comparisons were modelled using ANOVA with *post-hoc* comparisons made with the emmeans package_ENREF_26,[28] which included using least-squares linear models with pairwise comparisons and Tukey HSD correction for multiple comparisons where appropriate. Correlations between protein concentrations or ratios and motor disease severity (MDS-UPDRS part III) or disease duration (time from diagnosis) were performed using linear models. Age was included as a covariate in models where the biomarker concentration was associated with age with a *P*-value < 0.1. This was true for α-synuclein ($P = 0.05$), pTau181 ($P = 0.06$), pSer312-IRS-1 ($P = 0.06$), pY-IRS-1 ($P = 0.025$) and the α-synuclein/pTau ratio ($P = 0.01$) (Supplementary Fig. 3). We did not find any associations between IRS-1 biomarkers and body mass index (BMI; as one might have hypothesized); therefore, BMI was not included as a covariate in models for pSer312-IRS-1 or pY-IRS-1 (Supplementary Fig. 4).

To discriminate between groups, the pROC and precrec packages were used for receiver operating characteristic (ROC) and precision recall curves.[29,30] *P*-values for area under the curve for individual protein ROCs were generated through permeation tests. Proteins were included in a feature selection process using the Boruta method to identify the combinations that provided the highest discrimination between groups.[31,32] Important features were identified by maximizing AUC ROC through 5-fold cross-validation repeated 50 times. A similar cross-validation was used to estimate model performance. We report the linear discriminant analysis outcomes, but multiple classification algorithms were tested.

Data availability

Data are available upon request to the corresponding author.

Results

Demographics and cognition

Overall, Parkinson's disease individuals were younger compared to controls ($P < 0.001$). PD-CI individuals were older than PD-N individuals but were not different in age from controls ($P = 0.13$). When compared to PD-N, the control and PDD groups were older ($P < 0.001$ for both comparisons), while the PD-MCI group was not different ($P = 0.16$). PD-MCI individuals were younger than controls ($P = 0.02$) but PDD individuals and controls were similar in age ($P = 0.98$). PD-MCI individuals were younger than PDD individuals ($P = 0.008$) (Table 1).

Regarding cognitive performance by Montreal Cognitive Assessment (MoCA) scores, Parkinson's disease individuals had a lower average score compared to controls ($P < 0.001$). PD-CI individuals had a lower MoCA score than controls ($P < 0.001$) and PD-N individuals ($P < 0.001$). Compared to PD-N, MoCA scores of controls were not different ($P = 0.89$), but PD-MCI and PDD scored lower than PD-N ($P < 0.001$ for both comparisons). PD-MCI and PDD individuals scored lower than controls ($P < 0.001$ for both comparisons). PDD individuals scored lower than PD-MCI individuals ($P < 0.001$) (Table 1).

L1CAM+ NEV characterization

To characterize NEVs we used several methods with main results being presented in Figs 1 and 2. Cryo-TEM pictures of NEV preparations demonstrate two examples of small and medium size EVs with typical morphology appearing on the same frame; these pictures are consistent with isolation of a mixed population of exosomes and microvesicles (Fig. 1A and B). Nanoparticle tracking analysis shows a size distribution of particles typical of plasma EVs [mode across samples was 150.4 (20.6) nm; Fig. 1C]. NEVs are positive for intravesicular EV marker Alix and transmembrane EV markers CD9 and CD81, and negative for the *cis*-Golgi marker GM130 (Fig. 1D). To demonstrate the efficiency of the isolation methodology, we performed western blots with primary antibody against L1CAM loading L1CAM+ EVs, a surrogate of total plasma EVs isolated using a mix of anti-tetraspanin antibodies (i.e. CD9+/CD63+/CD81+ EVs), and eluates of beads only (Fig. 2A). L1CAM+ EVs display both 200 and 220 kDa characteristic bands (with the 220 kDa band being present in brain lysate), while CD9+/CD63+/CD81+ EVs and eluate of beads only display the 200 kDa band. This suggests that L1CAM+ EVs contain membrane-bound as well as soluble L1CAM, whereas other preparations contain only soluble L1CAM. The ratio of L1CAM/CD9 is higher for L1CAM+ EVs when compared to beads only or CD9+/CD63+/CD81+ EVs, suggesting specificity of the anti-L1CAM immunoprecipitation (Fig. 2A). To further address the issue of soluble versus EV-bound L1CAM, we developed a Homebrew SIMOA® intact L1CAM+ EV detection assay. We compared the eluates of using beads only; CD9+/CD63+/CD81+ EVs; L1CAM+ NEVs; and, as further negative control, EVs isolated using an antibody against ASGR2, a surface marker expressed in the liver and not expressed in the brain (ASGR2+ EVs) (https://www.proteinatlas.org/ENSG00000161944-ASGR2/tissue) ($n = 10$). Results demonstrate a many-fold higher yield of L1CAM+ EVs with the specific anti-L1CAM isolation compared to all other conditions (Fig. 2B). Next, we performed surface cargo analysis of L1CAM+ EVs by Exoview R200 and results show that L1CAM+ EVs express all major tetraspanins, that a majority of them express CD9 compared to CD81 and CD63, and that L1CAM co-localizes with EVs expressing all major tetraspanins (Fig. 2C and D). Finally, NEVs were further characterized by double immunolabelling with L1CAM and exosome marker Alix or L1CAM and neuronal EV marker Vamp2.[33] Using confocal fluorescence microscopy with Airyscan, we readily observed coexistence of L1CAM and Alix (Fig. 2E, left) and of L1CAM and Vamp2 (Fig. 2E, right) on particles at the size range of single EVs.

Figure 2 Continued
Using the same starting plasma samples ($n = 10$), we conducted parallel isolations, which differed in the immunoprecipitation step, in terms of using beads only; a mix of anti-tetraspanin antibodies (i.e. CD9+/CD63+/CD81+ EVs); the 5G3 clone of anti-CD171 antibody (i.e. L1CAM+ EVs); and, as further negative control, antibody against ASGR2, a surface marker not expressed in the brain (ASGR2+ EVs). Results demonstrate a many-fold higher yield of L1CAM+/tetraspanin+ EVs with the specific anti-L1CAM isolation compared to all other conditions. (**C**) Characteristic image from Exoview R200 analysis of L1CAM+ NEVs by using a modified ExoView Tetraspanin chip (antibodies against CD9, CD63 and CD81 for capture; fluorescent antibodies against CD9 and L1CAM for detection). (**D**) Pie charts demonstrate counts for particles captured by each tetraspanin and detected by CD9, L1CAM or both; the analysis demonstrates that L1CAM+ NEVs express all major tetraspanins, that a majority of them express CD9 compared to CD81 and CD63; and that L1CAM co-localizes with EVs expressing all major tetraspanins. (**E**) Representative confocal Airyscan fluorescence images of plasma EVs labelled with L1CAM (green) and Alix (magenta) or L1CAM (green) and neuronal marker Vamp2 (magenta). The enlarged views in boxes show examples of EVs co-labelled with L1CAM and Alix or Vamp2. *$P < 0.05$; **$P < 0.01$; ***$P < 0.001$.

Table 1 Participant demographics and clinical characteristics

	Control	PD	PD-N	PD-MCI	PDD	PD-CI	Significance Model: comparison
Sample size, *n*	49	224	103	81	40	121	
Male/female, *n*	28/21	156/68	65/38	58/23	33/7	91/30	
Age, years	75.8 (7.3)	71.8 (7.0)	69.9 (7.1)	72.0 (6.8)	76.2 (5.2)	73.4 (6.6)	1: PD < control***
							2: PD-N < control***
							2: PD-N < PD-CI***
							3: PD-N < PDD***
BMI	26.3 (4.0)	25.8 (4.2)	25.7 (4.3)	25.8 (4.2)	26.3 (4.4)	24.8 (3.5)	
Disease duration, years		9.3 (5.5)	8.3 (5.1)	10.0 (5.4)	10.1 (6.2)	10.0 (5.6)	2: PD-N < PD-CI*
Disease motor severity (MDS-UPDRS Part III)		39.5 (14.1)	34.1 (13.1)	43.5 (13.0)	47.8 (13.1)	44.8 (13.1)	2: PD-N < PD-CI***
							3: PD-N < PD-MCI***
							3: PD-N < PDD***
Disease stage, H & Y; median [min–max]		2.5 [1.0–5.0]	2.0 [1.0–3.0]	2.5 [1.0–5.0]	3.0 [2.0–5.0]	2.5 [1.0–5.0]	2: PD-N < PD-CI***
							3: PD-N < PD-MCI***
							3: PD-N < PDD***
LED, mg		898.5 (588.0)	805.5 (531.4)	1015.5 (637.7)	902.2 (595.5)	978.7 (624.0)	2: PD-N < PD-CI*
MoCA	26.9 (2.0)	23.6 (4.8)	26.5 (2.5)	23.2 (3.1)	16.6 (4.7)	21.0 (4.8)	1: Control > PD***
							2: PD-N > PD-CI***
							2: Control > PD-CI***
							3: PD-N > PD-MCI***
							3: PD-N > PDD***
							3: PD-MCI > PDD***
							3: Control > PD-MCI***
							3: Control > PDD***

Demographic information and clinical variables for Parkinson's disease individuals (further divided by cognitive groups PD-N, PD-CI, PD-MCI, and PDD) and cognitively normal controls. Values are presented as mean (SD) with median [min–max] for Hoehn and Yahr (H & Y). PD = Parkinson's disease; PD-N = PD normal cognition; PD-MCI = PD mild cognitive impairment; PDD = PD dementia; PD-Cognitive impairment (PD-CI = PD-MCI + PDD); BMI = body mass index; MDS-UPDRS Part III = Movement Disorder Society Unified Parkinson's Disease Rating Subscale Part III; LED = levodopa equivalent dose; MoCA = Montreal Cognitive Assessment. Hoehn and Yahr = 5 is related to patients being wheelchair-bound. Group differences were calculated using three least-squares linear models with pairwise comparisons and Tukey HSD correction for multiple comparisons where appropriate. Hoehn and Yahr were compared using the Kruskal–Wallis test with Dunn's test for pairwise comparisons with Bonferroni correction. Significant comparisons are listed, non-significant comparisons are not. Model 1: PD versus control; Model 2: PD-N versus PD-CI versus control; Model 3: PD-N versus PD-MCI versus PDD versus control.

*$P < 0.05$, **$P < 0.01$, ***$P < 0.001$.

Group differences in NEV cargo: Parkinson's/Alzheimer's disease pathogenic proteins

NEV α-synuclein (Fig. 3A) was lower in Parkinson's disease individuals than controls ($P = 0.004$). PD-CI individuals had lower α-synuclein compared to PD-N ($P < 0.001$) and controls ($P < 0.001$), while controls were not different from PD-N (Fig. 3B). Both PD-MCI and PDD individuals had significantly lower α-synuclein levels compared to PD-N ($P = 0.035$ and $P < 0.001$, respectively) and compared to controls ($P = 0.031$ and $P < 0.001$, respectively), while they did not differ from each other ($P = 0.27$) (Supplementary Fig. 5A).

NEV Aβ42 (Supplementary Fig. 6) levels were not different between Parkinson's disease and controls but showed a weak trend for higher levels in PD-CI than PD-N ($P = 0.08$).

NEV tTau (Supplementary Fig. 7) levels were not different between groups (with the caveat that many values were excluded due to high CVs).

NEV pTau181 (Fig. 4A) levels were higher in Parkinson's disease individuals than controls ($P = 0.003$). PD-CI individuals had higher NEV pTau181 levels than controls ($P = 0.001$) and a trend toward higher levels compared to PD-N ($P = 0.07$) (Fig. 4B). pTau181 of PD-MCI individuals was higher than that of controls ($P = 0.004$) but not of PD-N ($P = 0.12$). pTau181 of PDD individuals was higher than that of controls ($P = 0.045$) but not of PD-N ($P = 0.56$) (Supplementary Fig. 5B). pTau181 of controls was not different from that of PD-N ($P = 0.33$) and pTau181 also did not differ between PD-MCI and PDD individuals ($P = 0.98$) (Supplementary Fig. 5B).

The α-synuclein to pTau181 ratio (Supplementary Fig. 8A) was higher in controls compared to Parkinson's disease individuals ($P < 0.001$). Ratios in PD-CI individuals were lower than in PD-N ($P < 0.001$) (Supplementary Fig. 8B). Ratios in PD-MCI and PDD individuals were not different to ratios in PD-N ($P = 0.33$ and $P = 0.37$, respectively) and ratios in PD-MCI and PDD were lower than in controls ($P = 0.007$ and $P = 0.012$, respectively) (Supplementary Fig. 8C).

Group differences in NEV cargo: insulin signalling/mTOR biomarkers

NEV pSer312-IRS-1 (Supplementary Fig. 9) levels were not different between groups.

NEV pY-IRS-1 (Fig. 5A) was lower in Parkinson's disease individuals compared to controls ($P = 0.034$). PD-CI individuals had lower pY-IRS-1 compared to PD-N ($P = 0.021$) and controls ($P = 0.011$), while controls were not different from PD-N ($P = 0.10$) (Fig. 5B). PD-MCI individuals had lower pY-IRS-1 levels than controls ($P = 0.04$) and showed a trend for lower pY-IRS-1 than PD-N ($P = 0.08$) (Supplementary Fig. 5C); PDD individuals showed trends for lower pY-IRS-1 than controls ($P = 0.08$) and PD-N ($P = 0.07$); while PD-MCI and PDD did not differ from each other ($P = 1.0$) (Supplementary Fig. 5C).

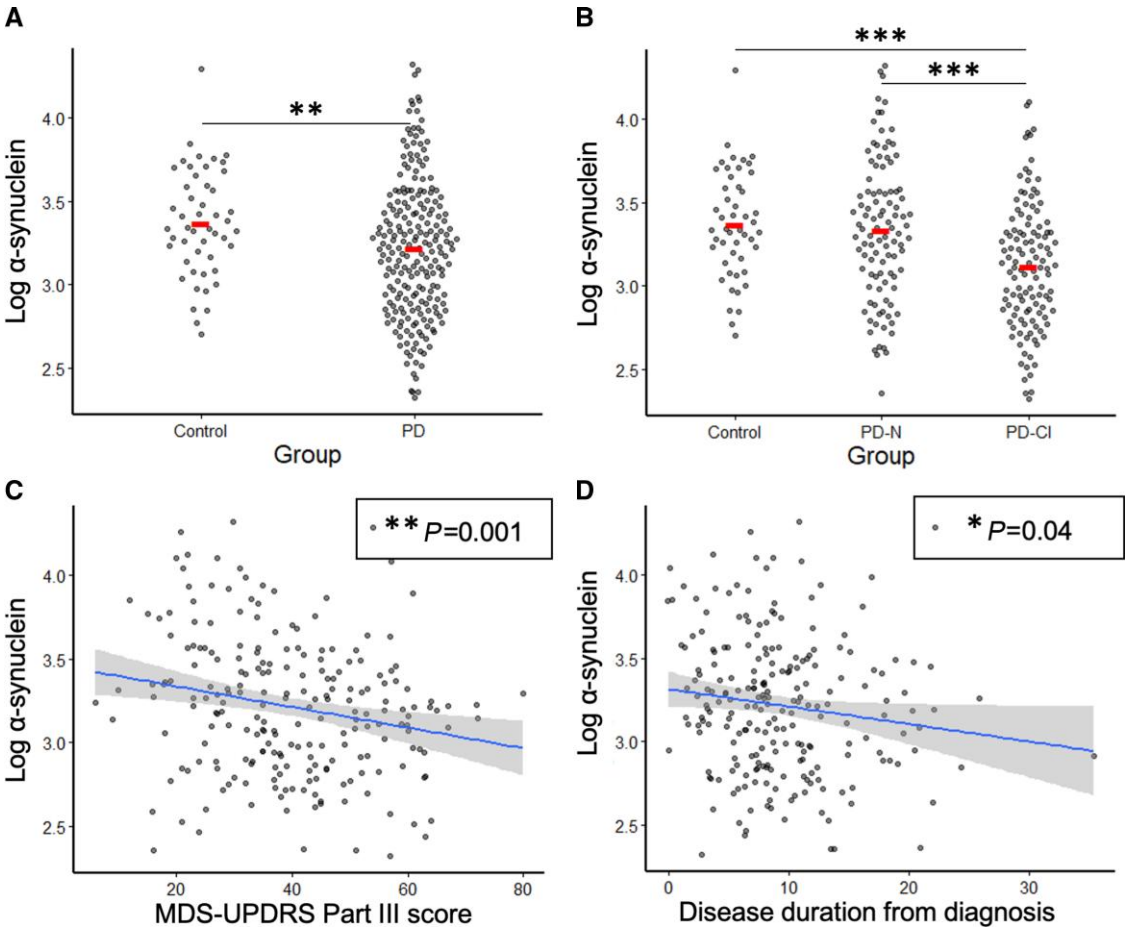

Figure 3 NEV levels of α-synuclein as a PD-CI biomarker. (**A** and **B**) NEV levels of total α-synuclein in healthy controls, individuals with Parkinson's disease (PD), individuals with Parkinson's disease and Normal cognition (PD-N) and individuals with Parkinson's disease and Cognitive Impairment (PD-CI = PD-MCI + PDD). Each point is representative of the value for an individual subject in each group and the horizontal red line is the mean level for that group. (**C** and **D**) NEV levels of α-synuclein in Parkinson's disease individuals against corresponding MDS-UPDRS part III indicating motor disease severity and disease duration from diagnosis (years). *P < 0.05; **P < 0.01; ***P < 0.001.

NEV mTOR (Supplementary Fig. 10) was not different between groups.

NEV pmTOR levels were not different between Parkinson's disease and controls (Supplementary Fig. 11A). PD-CI individuals showed a trend for lower pmTOR level than PD-N ($P = 0.06$) (Supplementary Fig. 11B). No differences were seen between PD-MCI or PDD and controls or PD-N (Supplementary Fig. 11C).

The ratio of pSer312-IRS-1 to pY-IRS-1 (Supplementary Fig. 12A) was higher in Parkinson's disease individuals compared to controls ($P = 0.034$). PD-CI individuals had a higher ratio compared to PD-N ($P = 0.02$) and controls ($P = 0.008$), while controls did not differ from PD-N (Supplementary Fig. 12B). The pSer312-IRS-1 to pY-IRS-1 ratio was higher in PD-MCI than PD-N and controls ($P = 0.037$ and $P = 0.015$, respectively) while it was not different between PDD and PD-N or between PD-MCI and PDD (Supplementary Fig. 12C).

Associations between clinical variables and NEV cargo

α-Synuclein was negatively associated with disease duration ($P = 0.04$) (Fig. 3D). α-Synuclein (Fig. 3C) and pY-IRS-1 (Fig. 5C) were negatively associated with motor disease severity as measured by MDS-UPDRS part III ($P = 0.001$ and $P = 0.003$, respectively), whereas pTau181 (Fig. 4C) was positively associated with motor disease severity ($P = 0.01$). The ratio of NEV pSer312-IRS-1 to pY-IRS-1 (Supplementary Fig. 12D) and the ratio of α-synuclein to pTau181 (Supplementary Fig. 8D) were also associated with motor disease severity ($P = 0.003$ and $P < 0.001$, respectively). The ratio of α-synuclein to pTau181 showed a trend for association with disease duration ($P = 0.06$, Supplementary Fig. 8E).

No NEV biomarkers were associated with LED.

NEV α-synuclein is more informative than plasma α-synuclein

To address the added value of measuring α-synuclein levels in NEVs as opposed to plasma, we measured α-synuclein in EV-depleted plasma in a randomly selected subcohort of Parkinson's disease patients and controls ($n = 73$). We found that both NEV and plasma α-synuclein was lower in PD-CI patients compared to controls ($P < 0.001$ and $P = 0.001$, respectively) (Supplementary Fig. 13A and B). Additionally, the NEV and plasma α-synuclein levels were highly intercorrelated (Supplementary Fig. 13C). However, NEV α-synuclein provided a better separation between groups [AUC for NEV α-synuclein = 0.772 (0.658–0.886) versus AUC for plasma α-synuclein = 0.696 (0.573–0.820)] (Supplementary Fig. 13D and E), which indicates that NEV α-synuclein is a more valuable measure than plasma α-synuclein.

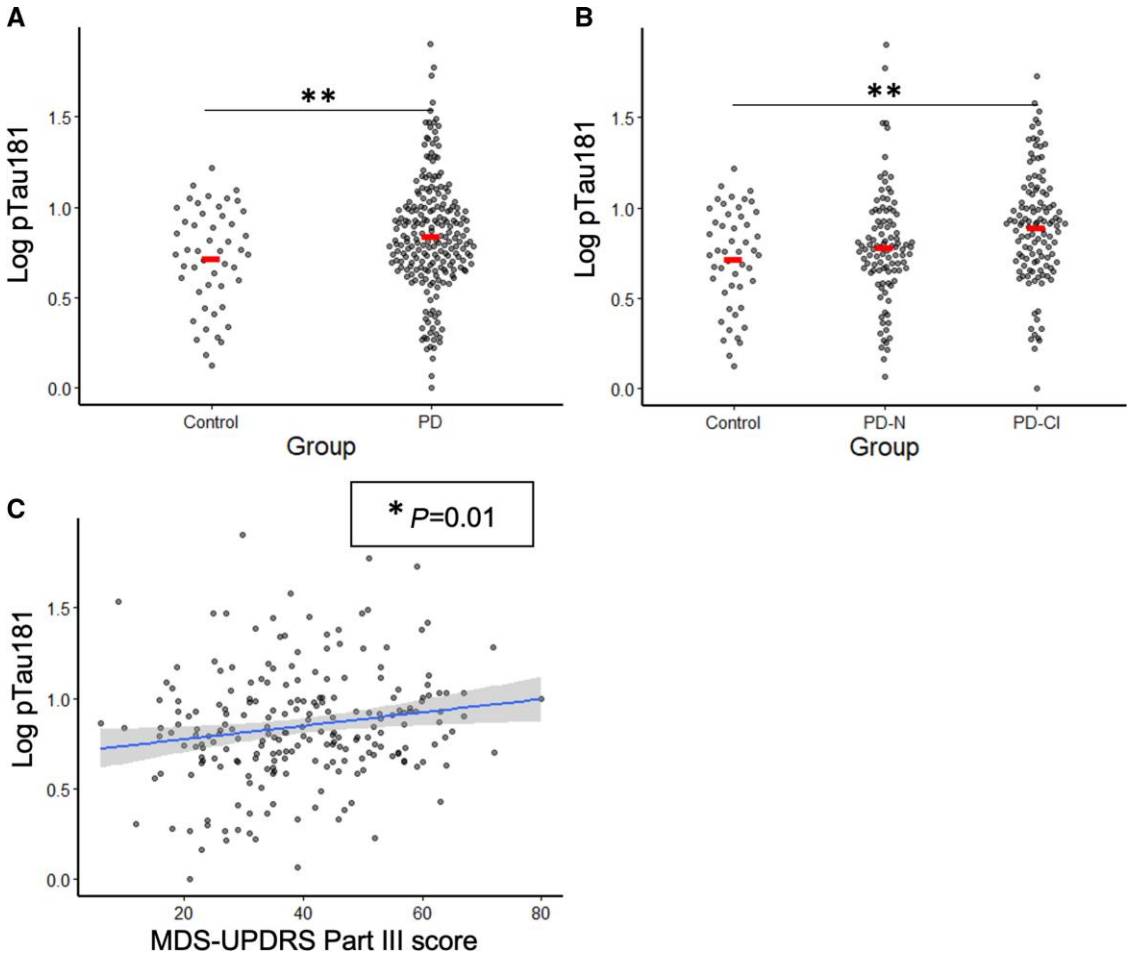

Figure 4 NEV levels of pTau 181 as a PD-CI biomarker. (**A** and **B**) NEV levels of pTau181 in healthy controls, individuals with Parkinson's disease (PD), individuals with Parkinson's disease and Normal cognition (PD-N) and individuals with Parkinson's disease and Cognitive Impairment (PD-CI = PD-MCI + PDD). Each point is representative of the value for an individual subject in each group and the horizontal red line is the mean level for that group. (**C** and **D**) NEV levels of α-synuclein in Parkinson's disease individuals against corresponding MDS-UPDRS part III indicating motor disease severity and disease duration from diagnosis (years). *$P < 0.05$; **$P < 0.01$; ***$P < 0.001$.

ROC analysis: NEV biomarkers in diagnostic classification

Results of ROC analyses are shown in Supplementary Figs 14 and 15 and Supplementary Tables 2 and 3 for Parkinson's disease versus controls and PD-N versus PD-CI. Among NEV biomarkers, α-synuclein, pTau181 and pmTOR were able to discriminate between control and Parkinson's disease individuals (AUC = 0.62, P = 0.005; AUC = 0.60, P = 0.02; AUC = 0.58, P = 0.04, respectively). Among Parkinson's disease individuals, PD-N could be discriminated from PD-CI by α-synuclein, pTau181, Aβ42, pY-IRS-1 and pmTOR (AUC = 0.65, $P < 0.001$; AUC = 0.62, P = 0.002; AUC = 0.59, P = 0.01; AUC = 0.63, $P < 0.001$; AUC = 0.57, P = 0.02, respectively). PD-N could be discriminated from PD-MCI (Supplementary Table 4) by α-synuclein, pTau181, Aβ42, pY-IRS-1 and pmTOR (AUC = 0.62, $P <$ 0.01; AUC= 0.62, $P < 0.01$; AUC = 0.59, $P < 0.05$; AUC = 0.62, $P < 0.01$; AUC = 0.59, $P < 0.05$, respectively) and from PDD (Supplementary Table 5) by α-synuclein, pY-IRS-1, pTau181, pSer312-IRS-1 and Aβ42 (AUC = 0.71, $P < 0.001$; AUC = 0.65, $P < 0.01$; AUC = 0.60, $P <$ 0.05; AUC = 0.59, $P < 0.05$; AUC = 0.59, P = 0.05, respectively). The feature selection analysis (Supplementary Fig. 16) resulted in important features being selected for all comparisons except for controls versus PD-N. The AUC values for the selected features are presented in Supplementary Table 6. The control versus Parkinson's disease (AUC = 0.60), PD-N versus PD-CI (AUC = 0.69), PD-N versus PD-MCI (AUC = 0.67) and PD-N versus PDD (AUC = 0.71) reached significance. α-Synuclein, pTau181 and pY-IRS-1 were consistently selected across all group comparisons.

Discussion

Summary

In the present study we showed that Parkinson's disease compared to control individuals had lower NEV levels of α-synuclein and pY-IRS-1, and higher levels of pTau181. Moreover, Parkinson's disease individuals with cognitive impairment exhibited lower NEV levels of α-synuclein and pY-IRS-1 and higher levels of pTau181 than cognitively intact Parkinson's disease individuals. Levels of α-synuclein, pTau181 and pY-IRS-1 were associated with Parkinson's disease motor symptom severity. Additionally, biomarker ratios of pSer312-IRS-1/pY-IRS-1 and α-synuclein/pTau181 differed between Parkinson's disease individuals and controls and between PD-N and PD-CI individuals and had inverse associations with Parkinson's disease motor symptom severity. Feature

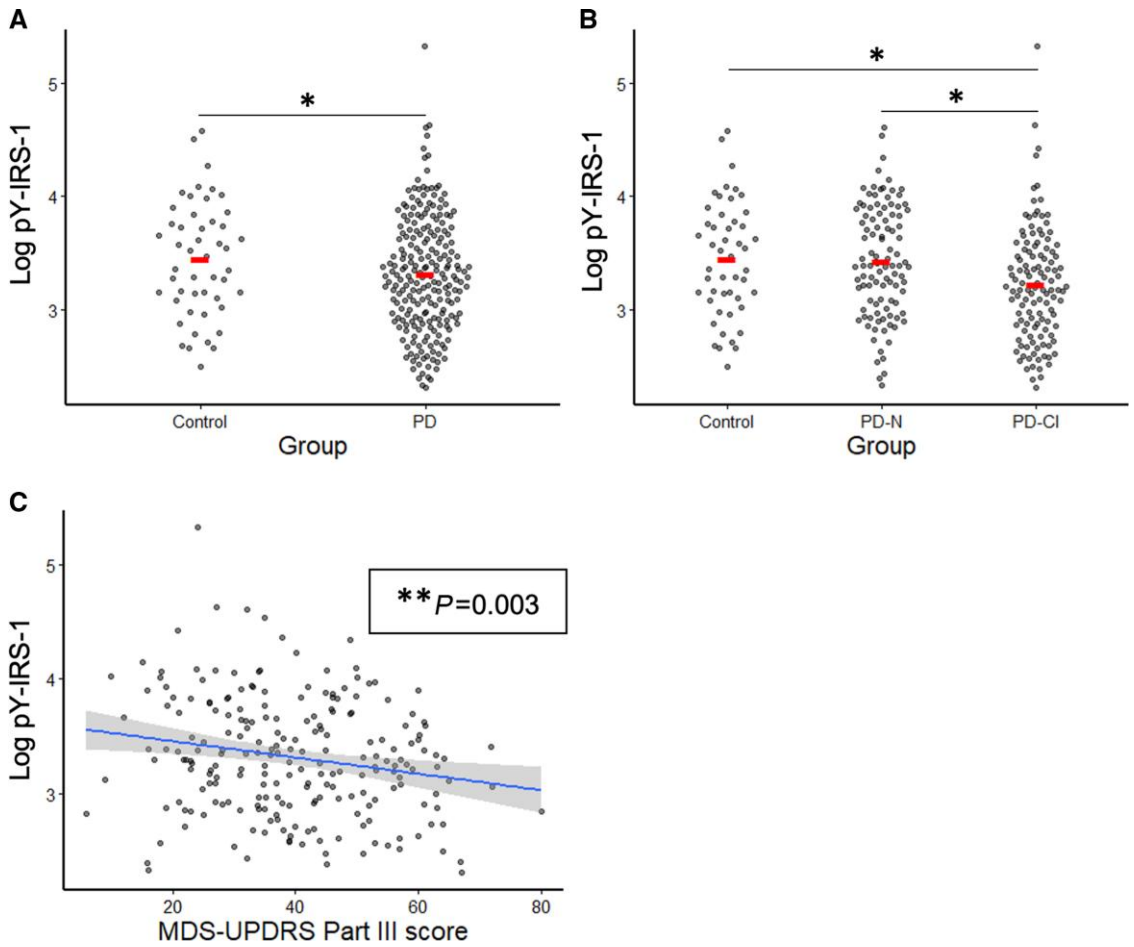

Figure 5 NEV levels of pY-IRS-1 as a PD-CI biomarker. (**A** and **B**) NEV levels of pY-IRS-1 in healthy controls, individuals with Parkinson's disease (PD), individuals with Parkinson's disease and normal cognition (PD-N) and individuals with Parkinson's disease and cognitive impairment (PD-CI = PD-MCI + PDD). Each point is representative of the value for an individual subject in each group and the horizontal red line is the mean level for that group. (**C** and **D**) NEV levels of α-synuclein in Parkinson's disease individuals against corresponding MDS-UPDRS part III indicating motor disease severity and disease duration from diagnosis (years). *P < 0.05; **P < 0.01; ***P < 0.001.

selection analysis showed that α-synuclein, pTau181 and pY-IRS-1 were consistently selected as important discriminants between Parkinson's disease and control individuals, as well as between cognitively impaired and unimpaired Parkinson's disease individuals. These novel findings support the view that aggregating proteins typically associated with Parkinson's disease (α-synuclein) and Alzheimer's disease (pTau181) are jointly involved in the pathogenesis of cognitive impairment in Parkinson's disease. Further, diminished insulin signalling propagation reflected in lower pY-IRS-1 availability seems to characterize cognitive impairment in Parkinson's disease and may broadly contribute to disease progression and severity.

NEV α-synuclein may decrease with cognitive impairment in Parkinson's disease

The aggregation of α-synuclein is the proximate cause of the degeneration of dopaminergic neurons in the substantia nigra pars compacta and other brain areas and is considered the hallmark pathology in Parkinson's disease. These pathological changes occur even before the onset of clinical symptoms in Parkinson's disease,[34,35] raising the possibility of preclinical diagnosis by biomarkers. EVs are implicated in the spread of pathogenic proteins in the brain, while also crossing the blood–brain barrier and thereby becoming measurable in the periphery.[12,36,37] This biomarker has shown inconsistent findings in EV studies (shown higher in Parkinson's disease in some studies[38,36,39] and lower in others[40–43]). A recent study using flow cytometry to analyse α-synuclein positivity of individual EVs reported decreased α-synuclein levels in CSF EVs in Parkinson's disease, an intriguing finding in light of the reported elevations in α-synuclein levels in plasma EVs by the same group.[41] In the present study, conducted blindly, we found lower NEV levels of α-synuclein in Parkinson's disease individuals compared to controls and a convincing stepwise decrease with cognitive impairment among Parkinson's disease individuals. In terms of biological plausibility, α-synuclein's progressive aggregation in neurons to form Lewy bodies or smaller aggregates could lead to decreased efflux of α-synuclein in EVs from neurons, and this decrease would be expected to become more prominent with progressive disease. Recent studies provide mechanistic proof of principle for the possibility that accumulation of intracellular α-synuclein may be reflected by decreased α-synuclein in secreted EVs. For instance, reduced ATP13A2 (an ATPase transporter highly expressed in the substantia nigra pars compacta[44]) levels result in >3-fold decrease in EV-associated α-synuclein, possibly due to impaired biogenesis of

α-synuclein-positive EVs,[45] while increasing intracellular α-synuclein.[46] The biological plausibility, agreement with recent reports utilizing advanced techniques[41] and the fact that all assessments were conducted blindly collectively inspire confidence in the validity of our findings concerning α-synuclein.

NEVs reflect mixed neuropathologies in Parkinson's disease

As is common for neurodegenerative diseases,[47] Parkinson's disease often involves mixed pathologies that may relate to symptom variability, ranging from pure motor symptoms to motor impairment with overt dementia. It is hypothesized that a synergistic relationship occurs between aggregation-prone proteins Aβ, tau and α-synuclein.[48] A clinicopathological study in Parkinson's disease and PDD cases found that a combination of α-synuclein, Aβ and tau was a better predictor of dementia than the severity of any single pathology, while cortical Aβ and Braak tau staging were better predictors of worse ante-mortem cognition than α-synuclein pathology.[49,50] Importantly, pathologically confirmed cases of Alzheimer's disease, dementia with Lewy bodies and PDD show distinct patterns of cognitive impairment including different rates of decline across memory and executive function domains.[51] CSF studies have generally found decreased levels of Aβ42 and increased levels of pTau and tTau in Parkinson's disease compared to controls and associations with disease severity.[52–54] PET studies have explored baseline and longitudinal changes in the levels of aggregating proteins across the Parkinson's disease spectrum yielding mixed results for the role of these proteins, especially when considered individually.[55–60] One study revealed that, among PD-N and PD-MCI individuals, tau PET binding was significantly elevated in Aβ-positive individuals, but, surprisingly, cognitive deficits were not associated with advanced Aβ or tau pathology.[60] In general, Aβ PET studies have not demonstrated robust associations between Aβ PET ligand binding and cognitive impairment in Parkinson's disease. For instance, Florbetaben PET was unable to distinguish between PDD, PD-MCI and PD-N, although increased baseline amyloid burden may be associated with higher risk for future cognitive impairment.[58,60] Therefore, the literature at large is in agreement with our finding that NEV Aβ42 levels were not associated cross-sectionally with Parkinson's disease and cognitive impairment, whereas pTau181 levels were robustly associated with both. In the field of Alzheimer's disease, it is now widely accepted that pTau181 is a marker of tauopathy, whereas tTau is a rather non-specific marker of neurodegeneration.[61,62] Moreover, we have repeatedly found that pTau181 in NEVs is a much better biomarker for clinical and preclinical AD than tTau,[14,16] a pattern that was also observed by the present study in the setting of Parkinson's disease. Altogether, our findings suggest that multiple underlying pathologies may act additively or, perhaps, synergistically to produce cognitive impairment in Parkinson's disease.

An interesting aspect of our findings is that NEV α-synuclein levels were lower, but pTau181 levels were higher in Parkinson's disease individuals compared to controls, while their respective directions of association with motor disease severity were opposite. *In vitro* examination of Tau and α-synuclein have demonstrated that α-synuclein and tau monomers facilitate each other's fibrillation and co-aggregation.[63] One recent study suggested that α-synuclein phosphorylation triggers pathogenic tau in neurons, but pTau had more severe pathology spread in post-mortem Parkinson's disease brains.[64] However, the sorting of tau and α-synuclein into EVs may be governed by different mechanisms and their changes with cognitive impairment in Parkinson's disease require further study. The ratio of α-synuclein to pTau181 in our study was significantly different in all models for group comparisons (Models 1, 2, and 3; Supplementary Fig. 8). This ratio is a metric that merits further exploration in Parkinson's disease, with the potential for biomarker use similar to the protein ratio of Aβ/pTau in Alzheimer's disease. In our study, the α-synuclein to pTau181 ratio accentuates the association of cognition with pathogenic protein concentrations and highlights the synergistic relationship between these proteins in Parkinson's disease individuals.

NEVs may reflect impaired feed-forward brain insulin signalling in Parkinson's disease

Insulin resistance and Parkinson's disease have long been linked to each other, but the mechanisms explaining their relationship remain only partially understood.[65,66] Peripheral insulin resistance and glucose metabolism abnormalities are more prevalent in Parkinson's disease and PDD individuals compared to healthy controls, with insulin resistance being present in 35% of Parkinson's disease individuals, but 62% of PDD individuals.[67] Another recent study reported that about 60% of Parkinson's disease individuals show insulin resistance by HOMA-IR, despite normal blood sugar levels.[68] In addition, insulin resistance has been observed in nigral neurons in post-mortem brain tissue of Parkinson's disease patients.[9] At the molecular level, IRS-1 phosphorylations determine the efficiency of insulin signalling and the emergence of insulin resistance.[69] Generally, increased serine and decreased tyrosine phosphorylations result in decreased IRS-1 binding and activation of downstream substrates phosphatidylinositol 3-kinase and Akt (protein kinase B).[69,70] Decreased levels of tyrosine-phosphorylated IRS-1 has also been linked with neurodegenerative diseases like Alzheimer's disease and Parkinson's disease.[18,71,72] In the present study, we evaluated both tyrosine and serine IRS-1 phosphorylations in NEVs, to respectively assess both forward signalling along the cascade and insulin resistance (as pSer312-IRS-1 levels are determined by various kinases involved in feedback loops aiming to restrict excessive insulin signalling). Our finding of decreased pY-IRS-1 NEV levels in Parkinson's disease individuals compared to controls, and lower levels in PD-CI compared to PD-N individuals suggest deficient neuronal forward insulin signalling in Parkinson's disease, while similar pSer312 levels across groups perhaps indicate a lesser problem with insulin resistance. These results are in agreement with our earlier findings on NEV biomarkers from the exenatide Parkinson's disease trial; we found a substantial increase in NEV pY-IRS-1 in exenatide-treated compared to placebo-treated participants after 48 weeks of treatment, which persisted even after a 12-week washout period, and was associated with motor symptom improvement, while pSer312-IRS-1 levels remained unchanged with exenatide.[15] Our finding that lower NEV pY-IRS-1 levels are associated with higher motor symptom severity in Parkinson's disease suggest that decreasing pY-IRS-1 is contributing to worsening Parkinson's disease and that elevating it (such as by exenatide) may offer disease-modifying benefits.

The canonical insulin signalling cascade induces mTOR phosphorylation and activation, a known neuroprotective mechanism.[73,74] Therefore, we explored whether decreased insulin signalling would also lead to decreased mTOR phosphorylation, although the effect would be expected to be 'diluted' by the effects of many unaccounted cascades influencing mTOR. This may explain why, in this study, group differences between Parkinson's disease and controls were modest and only significant for the comparison

between PD-MCI and PD-N,[64] whereas, in the exenatide Parkinson's disease study, NEV pmTOR levels showed modest elevations with exenatide treatment.

Limitations and strengths

Limitations of the study include a significant difference in age between control and Parkinson's disease groups, where the specific recruitment strategy resulted in PDD being age-matched to controls, although this was addressed by including age as a covariate in all analyses. Reported results have not been corrected for multiple comparisons, although some key results would have even survived Bonferroni correction (i.e. group differences for pTau181 and α-synuclein would have even met a significance level of 0.00625, appropriate when measuring and comparing 8 individual analytes). In addition, besides the main comparison between controls, PD-N and PD-CI groups, which represents the main focus of the study, we also performed comparisons for additional subgroupings: between controls and PD groups, which is likely of interest to most readers, as well as between controls, PD-N, PD-MCI and PD-D groups, as exploratory. These results derived from a single cohort require validation and replication in larger multicentre cohorts and further evaluation of their biological plausibility. The strengths of this study include a well-characterized cohort, which allowed us to examine associations of NEV biomarkers with diverse clinical measures. Moreover, NEV isolations and biomarker determinations were conducted blindly regarding group membership.

Conclusions

Taken together, our results hint at a potential synergistic relationship between pTau and α-synuclein in producing cognitive impairment in Parkinson's disease, which warrants further inquiry. Future studies examining longitudinal changes in NEV biomarkers of Parkinson's disease individuals who convert from PD-N to PD-MCI or PDD are needed to establish the relative timeline of biomarker changes in Parkinson's disease. Additionally, group differences for IRS-1 phosphoproteins reflect deficient forward insulin signalling in neurons and offer a mechanistic explanation to earlier findings of the effects of exenatide in Parkinson's disease. It would be interesting to examine how NEV IRS-1 phosphoproteins are related to brain glucose metabolism measured by FDG PET. Furthermore, this study confirms that NEVs are a valuable new tool for studying in parallel multiple pathogenic processes involved in the pathogenesis of neurodegenerative diseases. The identification of the underlying biology at the individual level (fingerprint) carries a tremendous potential for patient selection and stratification in disease-modification trials and for personalized medicine once specific treatments for the involved biological processes become available.

Acknowledgements

We acknowledge the contribution of Dr Anto Praveen Rajkumar Rajamani from the University of Nottingham and the Nanoscale and Microscale Research Centre of the University of Nottingham in acquiring the Cryo-TEM image in Fig. 1A.

Funding

This research was supported in part by the Intramural Research Program of the National Institute on Aging, National Institutes of Health. Data collection for the New Zealand Parkinson's Progression Programme was supported by the New Zealand Health Research Council (14/440), Lottery Health Research and Brain Research New Zealand.

Competing interests

The authors report no competing interests and have no conflicts of interest.

Supplementary material

Supplementary material is available at *Brain* online.

References

1. Jankovic J. Parkinson's disease: Clinical features and diagnosis. *J Neurol Neurosurg Psychiatry*. 2008;79:368–376.
2. Tysnes OB, Storstein A. Epidemiology of Parkinson's disease. *J Neural Transm (Vienna)*. 2017;124:901–905.
3. Braak H, de Vos RA, Jansen EN, Bratzke H, Braak E. Neuropathological hallmarks of Alzheimer's and Parkinson's diseases. *Prog Brain Res*. 1998;117:267–285.
4. Lang AE. The progression of Parkinson disease: A hypothesis. *Neurology*. 2007;68:948–952.
5. Svenningsson P, Westman E, Ballard C, Aarsland D. Cognitive impairment in patients with Parkinson's disease: Diagnosis, biomarkers, and treatment. *Lancet Neurol*. 2012;11:697–707.
6. Irwin DJ, Lee VM, Trojanowski JQ. Parkinson's disease dementia: Convergence of alpha-synuclein, tau and amyloid-beta pathologies. *Nat Rev Neurosci*. 2013;14:626–636.
7. Jellinger K, Braak H, Braak E, Fischer P. Alzheimer lesions in the entorhinal region and isocortex in Parkinson's and Alzheimer's diseases. *Ann N Y Acad Sci*. 1991;640:203–209.
8. Irwin DJ, Hurtig HI. The contribution of tau, amyloid-beta and alpha-synuclein pathology to dementia in Lewy body disorders. *J Alzheimers Dis Parkinsonism*. 2018;8:444.
9. Bassil F, Delamarre A, Canron M-H, *et al*. Impaired brain insulin signalling in Parkinson's disease. *Neuropathol Appl Neurobiol*. 2022;48:e12760.
10. van Niel G, D'Angelo G, Raposo G. Shedding light on the cell biology of extracellular vesicles. *Nat Rev Mol Cell Biol*. 2018;19:213–228.
11. Hill AF. Extracellular vesicles and neurodegenerative diseases. *J Neurosci*. 2019;39:9269–9273.
12. Thompson AG, Gray E, Heman-Ackah SM, *et al*. Extracellular vesicles in neurodegenerative disease—Pathogenesis to biomarkers. *Nat Rev Neurol*. 2016;12:346–357.
13. Mustapic M, Eitan E, Werner JK Jr, *et al*. Plasma extracellular vesicles enriched for neuronal origin: A potential window into brain pathologic processes. *Front Neurosci*. 2017;11:278.
14. Fiandaca MS, Kapogiannis D, Mapstone M, *et al*. Identification of preclinical Alzheimer's disease by a profile of pathogenic proteins in neurally derived blood exosomes: A case-control study. *Alzheimers Dement*. 2015;11:600–607.e1.
15. Athauda D, Gulyani S, Karnati HK, *et al*. Utility of neuronal-derived exosomes to examine molecular mechanisms that affect motor function in patients with Parkinson disease: A secondary analysis of the exenatide-PD trial. *JAMA Neurol*. 2019;76:420–429.
16. Kapogiannis D, Mustapic M, Shardell MD, *et al*. Association of extracellular vesicle biomarkers with Alzheimer disease in the

Baltimore longitudinal study of aging. *JAMA Neurol*. 2019;76: 1340–1351.
17. Eren E, Hunt JFV, Shardell M, *et al*. Extracellular vesicle biomarkers of Alzheimer's disease associated with sub-clinical cognitive decline in late middle age. *Alzheimers Dement*. 2020;16: 1293–1304.
18. Talbot K, Wang HY, Kazi H, *et al*. Demonstrated brain insulin resistance in Alzheimer's disease patients is associated with IGF-1 resistance, IRS-1 dysregulation, and cognitive decline. *J Clin Invest*. 2012;122:1316–1338.
19. Litvan I, Goldman JG, Tröster AI, *et al*. Diagnostic criteria for mild cognitive impairment in Parkinson's disease: Movement Disorder Society Task Force guidelines. *Mov Disord*. 2012;27: 349–356.
20. Emre M, Aarsland D, Brown R, *et al*. Clinical diagnostic criteria for dementia associated with Parkinson's disease. *Mov Disord*. 2007; 22:1689–1707; quiz 1837.
21. Tomlinson CL, Stowe R, Patel S, Rick C, Gray R, Clarke CE. Systematic review of levodopa dose equivalency reporting in Parkinson's disease. *Mov Disord*. 2010;25:2649–2653.
22. Wood KL, Myall DJ, Livingston L, *et al*. Different PD-MCI criteria and risk of dementia in Parkinson's disease: 4-year longitudinal study. *NPJ Parkinsons Dis*. 2016;2:15027.
23. Horne KL, MacAskill MR, Myall DJ, *et al*. Neuropsychiatric symptoms are associated with dementia in Parkinson's disease but not predictive of it. *Mov Disord Clin Pract*. 2021;8:390–399.
24. Nizamudeen Z, Markus R, Lodge R, *et al*. Rapid and accurate analysis of stem cell-derived extracellular vesicles with super resolution microscopy and live imaging. *Biochim Biophys Acta Mol Cell Res*. 2018; 1865:1891–1900.
25. Nizamudeen ZA, Xerri R, Parmenter C, *et al*. Low-power sonication can alter extracellular vesicle size and properties. *Cells*. 2021;10:2413.
26. Mondal A, Ashiq KA, Phulpagar P, Singh DK, Shiras A. Effective visualization and easy tracking of extracellular vesicles in glioma cells. *Biol Proced Online*. 2019;21:4.
27. Wickham H. *ggplot2: Elegant graphics for data analysis*. Springer.
28. Lenth RV, Buerkner P, Herve M, Love J, Riebl H, Singmann H. Estimated marginal means, aka least-squares means. CRAN.R-project.
29. Robin X, Turck N, Hainard A, *et al*. pROC: An open-source package for R and S+ to analyze and compare ROC curves. *BMC Bioinformatics*. 2011;12:77.
30. Saito T, Rehmsmeier M. Precrec: Fast and accurate precision–recall and ROC curve calculations in R. *Bioinformatics*. 2016;33:145–147.
31. Kursa MB, Jankowski A, Rudnicki WR. Boruta—A system for feature selection. *Fundamenta Inform*. 2010;101:271–285.
32. Kursa MB, Rudnicki WR. Feature selection with the Boruta package. *J Stat Software*. 2010;36:13.
33. Vilcaes AA, Chanaday NL, Kavalali ET. Interneuronal exchange and functional integration of synaptobrevin via extracellular vesicles. *Neuron*. 2021;109:971–983.e5.
34. Braak H, Del Tredici K, Rüb U, de Vos RA, Jansen Steur EN, Braak E. Staging of brain pathology related to sporadic Parkinson's disease. *Neurobiol Aging*. 2003;24:197–211.
35. Simunovic F, Yi M, Wang Y, *et al*. Gene expression profiling of substantia nigra dopamine neurons: Further insights into Parkinson's disease pathology. *Brain*. 2009;132(Pt 7):1795–1809.
36. Shi M, Liu C, Cook TJ, *et al*. Plasma exosomal α-synuclein is likely CNS-derived and increased in Parkinson's disease. *Acta Neuropathol*. 2014;128:639–650.
37. Shi M, Sheng L, Stewart T, Zabetian CP, Zhang J. New windows into the brain: Central nervous system-derived extracellular vesicles in blood. *Prog Neurobiol*. 2019;175:96–106.
38. Niu M, Li Y, Li G, *et al*. A longitudinal study on α-synuclein in plasma neuronal exosomes as a biomarker for Parkinson's disease development and progression. *Eur J Neurol*. 2020;27:967–974.
39. Jiang C, Hopfner F, Berg D, *et al*. Validation of α-synuclein in L1CAM-immunocaptured exosomes as a biomarker for the stratification of Parkinsonian syndromes. *Mov Disord*. 2021;36: 2663–2669.
40. Stuendl A, Kunadt M, Kruse N, *et al*. Induction of α-synuclein aggregate formation by CSF exosomes from patients with Parkinson's disease and dementia with Lewy bodies. *Brain*. 2015;139:481–494.
41. Hong Z, Tian C, Stewart T, *et al*. Development of a sensitive diagnostic assay for Parkinson disease quantifying α-synuclein-containing extracellular vesicles. *Neurology*. 2021; 96:e2332–e2345.
42. Si X, Tian J, Chen Y, Yan Y, Pu J, Zhang B. Central nervous system-derived exosomal alpha-synuclein in serum may be a biomarker in Parkinson's sisease. *Neuroscience*. 2019;413:308–316.
43. Chung C-C, Chan L, Chen J-H, Hung Y-C, Hong C-T. Plasma extracellular vesicle α-synuclein level in patients with Parkinson's disease. *Biomolecules*. 2021;11:744.
44. Ramirez A, Heimbach A, Gründemann J, *et al*. Hereditary parkinsonism with dementia is caused by mutations in ATP13A2, encoding a lysosomal type 5 P-type ATPase. *Nat Genet*. 2006;38: 1184–1191.
45. Kong SM, Chan BK, Park J-S, *et al*. Parkinson's disease-linked human PARK9/ATP13A2 maintains zinc homeostasis and promotes α-synuclein externalization via exosomes. *Hum Mol Genet*. 2014;23:2816–2833.
46. Usenovic M, Tresse E, Mazzulli JR, Taylor JP, Krainc D. Deficiency of ATP13A2 leads to lysosomal dysfunction, α-synuclein accumulation, and neurotoxicity. *J Neurosci*. 2012;32:4240–4246.
47. McAleese KE, Colloby SJ, Thomas AJ, *et al*. Concomitant neurodegenerative pathologies contribute to the transition from mild cognitive impairment to dementia. *Alzheimers Dement*. 2021;17:1121–1133.
48. Goedert M, Spillantini MG, Del Tredici K, Braak H. 100 years of Lewy pathology. *Nat Rev Neurol*. 2013;9:13–24.
49. Compta Y, Parkkinen L, O'Sullivan SS, *et al*. Lewy- and Alzheimer-type pathologies in Parkinson's disease dementia: Which is more important? *Brain*. 2011;134(Pt 5):1493–1505.
50. Kempster PA, O'Sullivan SS, Holton JL, Revesz T, Lees AJ. Relationships between age and late progression of Parkinson's disease: A clinico-pathological study. *Brain*. 2010; 133(Pt 6): 1755–1762.
51. Jellinger KA, Korczyn AD. Are dementia with Lewy bodies and Parkinson's disease dementia the same disease? *BMC Med*. 2018;16:34.
52. Dolatshahi M, Pourmirbabaei S, Kamalian A, Ashraf-Ganjouei A, Yaseri M, Aarabi MH. Longitudinal alterations of alpha-synuclein, amyloid beta, total, and phosphorylated tau in cerebrospinal fluid and correlations between their changes in Parkinson's disease. *Front Neurol*. 2018;9:560.
53. Irwin DJ, Fedler J, Coffey CS, *et al*. Evolution of Alzheimer's disease cerebrospinal fluid biomarkers in early Parkinson's disease. *Ann Neurol*2020;88:574–587.
54. Kang J. Cerebrospinal fluid amyloid β1-42, tau, and alpha-synuclein predict the heterogeneous progression of cognitive dysfunction in Parkinson's disease. *J Mov Disord*. 2016;9:89–96.
55. Gomperts SN, Locascio JJ, Rentz D, *et al*. Amyloid is linked to cognitive decline in patients with Parkinson disease without dementia. *Neurology*. 2013;80:85–91.

56. Gomperts SN, Marquie M, Locascio JJ, Bayer S, Johnson KA, Growdon JH. PET radioligands reveal the basis of dementia in Parkinson's disease and dementia with Lewy bodies. *Neurodegener Dis*. 2016;16:118–24.
57. Mashima K, Ito D, Kameyama M, *et al*. Extremely low prevalence of amyloid positron emission tomography positivity in Parkinson's disease without dementia. *Eur Neurol*. 2017;77:231–237.
58. Melzer TR, Stark MR, Keenan RJ, *et al*. Beta amyloid deposition is not associated with cognitive impairment in Parkinson's disease. *Front Neurol*. 2019;10:391.
59. Petrou M, Dwamena BA, Foerster BR, *et al*. Amyloid deposition in Parkinson's disease and cognitive impairment: A systematic review. *Mov Disord*. 2015;30:928–935.
60. Winer JR, Maass A, Pressman P, *et al*. Associations between tau, beta-amyloid, and cognition in Parkinson disease. *JAMA Neurol*. 2018;75:227–235.
61. Jack CR J, Bennett DA, Blennow K, *et al*. NIA-AA Research Framework: Toward a biological definition of Alzheimer's disease. *Alzheimers Dement*. 2018;14:535–562.
62. Jack CR J, Bennett DA, Blennow K, *et al*. A/T/N: An unbiased descriptive classification scheme for Alzheimer disease biomarkers. *Neurology*. 2016;87:539–547.
63. Lu J, Zhang S, Ma X, *et al*. Structural basis of the interplay between alpha-synuclein and tau in regulating pathological amyloid aggregation. *J Biol Chem*. 2020;295:7470–7480.
64. Hadi F, Akrami H, Totonchi M, Barzegar A, Nabavi SM, Shahpasand K. α-Synuclein abnormalities trigger focal tau pathology, spreading to various brain areas in Parkinson disease. *J Neurochemistry*. 2021;157:727–751.
65. Aviles-Olmos I, Limousin P, Lees A, Foltynie T. Parkinson's disease, insulin resistance and novel agents of neuroprotection. *Brain*. 2013;136(Pt 2):374–384.
66. Sandyk R. The relationship between diabetes mellitus and Parkinson's disease. *Int J Neurosci*. 1993;69:125–130.
67. Bosco D, Plastino M, Cristiano D, *et al*. Dementia is associated with insulin resistance in patients with Parkinson's disease. *J Neurol Sci*. 2012;315:39–43.
68. Hogg E, Athreya K, Basile C, Tan EE, Kaminski J, Tagliati M. High prevalence of undiagnosed insulin resistance in non-diabetic subjects with Parkinson's disease. *J Parkinsons Dis*. 2018;8:259–265.
69. Rask-Madsen C, Kahn CR. Tissue-specific insulin signaling, metabolic syndrome, and cardiovascular disease. *Arterioscler Thromb Vasc Biol*. 2012;32:2052–2059.
70. Gual P, Le Marchand-Brustel Y, Tanti JF. Positive and negative regulation of insulin signaling through IRS-1 phosphorylation. *Biochimie*. 2005;87:99–109.
71. Gao S, Duan C, Gao G, Wang X, Yang H. Alpha-synuclein overexpression negatively regulates insulin receptor substrate 1 by activating mTORC1/S6K1 signaling. *Int J Biochem Cell Biol*. 2015;64:25–33.
72. Sekar S, Taghibiglou C. Elevated nuclear phosphatase and tensin homolog (PTEN) and altered insulin signaling in substantia nigral region of patients with Parkinson's disease. *Neurosci Lett*. 2018;666:139–143.
73. Xu Y, Liu C, Chen S, *et al*. Activation of AMPK and inactivation of Akt result in suppression of mTOR-mediated S6K1 and 4E-BP1 pathways leading to neuronal cell death in in vitro models of Parkinson's disease. *Cell Signal*. 2014;26:1680–1689.
74. Zhu Z, Yang C, Iyaswamy A, *et al*. Balancing mTOR signaling and autophagy in the treatment of Parkinson's disease. *Int J Mol Sci*. 2019;20:728.